Mechanism of the Cooperative Adsorption of Oppositely Charged Nanoparticles†

Konstantin V. Tretiakov,‡ Kyle J. M. Bishop,‡ Bartlomiej Kowalczyk,‡ Archana Jaiswal,|| Mark A. Poggi,|| and Bartosz A. Grzybowski*,‡,§

Department of Chemical and Biological Engineering and Department of Chemistry, Northwestern University, 2145 Sheridan Road, Evanston, Illinois 60208, and Q-Sense, 808 Landmark Drive, Suite 124, Glen Burnie, Maryland 21061

Received: October 24, 2008; Revised Manuscript Received: December 24, 2008

Quartz crystal microbalance experiments were performed to study the kinetics of surface adsorption from solutions containing oppositely charged nanoparticles. A theoretical model was developed according to which formation of dense nanoparticle (NP) monolayers is driven by a cooperative process, in which the already-adsorbed NPs facilitate adsorption of NPs from solution. The kinetic rate constants change with the NP solution concentration and can be used to backtrack adsorption free energies. These energies agree with the predictions of a simple DLVO model.

Introduction

In the past decade, monolayers of inorganic nanoparticles deposited on various substrates have been studied extensively in the context of their potential applications in quantum dot light-emitting devices,[1] displays,[2] antireflective films,[3] corrosion protection,[4] heterogeneous catalysis,[5] and others. Although many methods exist to form monolayer NP films via chemical ligation,[6,7] electrodeposition,[8,9] Langmuir−Blodgett[10,11] or sol−gel[12] techniques, they are usually substrate-specific and often not easily scalable to large and/or curved surfaces. Recently, we reported a method that deposits monolayer NP coatings[13] (Figure 1) onto a range of materials including glasses, polymers, elastomers, and semiconductors. In this method, the NPs adsorb from aqueous solutions containing oppositely charged nanoparticles onto surfaces bearing residual charge, typically introduced by plasma oxidation. Remarkably, while neither positively charged nor negatively charged particles alone absorb onto the substrates, their mixtures adsorb cooperatively and deposit layers stabilized by favorable electrostatic interactions between oppositely charged NPs. The coatings thus deposited are stable against prolonged (weeks) soaking in water, salt solutions (<1 M), dilute acids and bases, as well as common organic solvents. The practically appealing features of this method are its simplicity and generality, ability to coat large areas and nonplanar surfaces, flexibility in tailoring surface composition (by using NPs of different types of cores), and the reusability of the plating solutions.

Herein, we study the kinetic mechanism that governs the adsorption process. Using the quartz crystal microbalance (QCM) technique, we obtain the kinetic data for the adsorption of NPs from solutions of different concentrations. The model we develop to reproduce the experimental trends highlights the importance of cooperative interactions between oppositely charged NPs and provides a generic mathematical framework with which to treat cooperative adsorption kinetics based on electrostatic interactions. Adsorption free energies estimated from the experimental data agree with those obtained directly from the DLVO theory. The most counterintuitive finding from these studies is that increasing the concentration of NPs in solution can decrease the rate of coating formation. This trend can be explained by the increased Debye screening and concomitant weakening of interactions between particles adsorbed from more concentrated solutions.

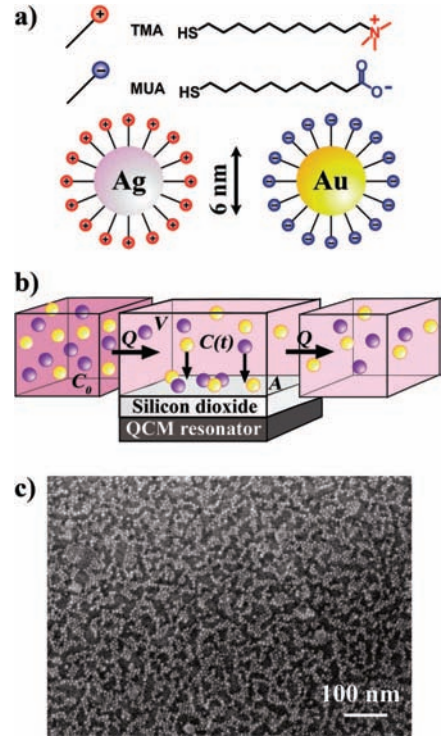

Figure 1. (a) Schematic representation of the *N,N,N*-trimethyl(11-mercaptoundecyl)ammonium chloride and mercaptoundecanoic acid thiols and of the charged NPs used in experiments. (b) Experimental arrangement. A mixture of oppositely charged NPs is flown through a QCM chamber of volume V at a flow rate Q. The NPs adsorb onto a plasma-oxidized SiO_2 surface of area A. Other quantities are defined in the main text when discussing the mass balance through the cell. (c) An SEM image of a typical NP coating deposited onto SiO_2.

† Part of the George C. Schatz Festschrift.

* Corresponding author. E-mail: grzybor@northwestern.edu.
‡ Department of Chemical and Biological Engineering, Northwestern University.
§ Department of Chemistry, Northwestern University.
|| Q-Sense.

10.1021/jp809447m CCC: $40.75
Published on Web 02/19/2009

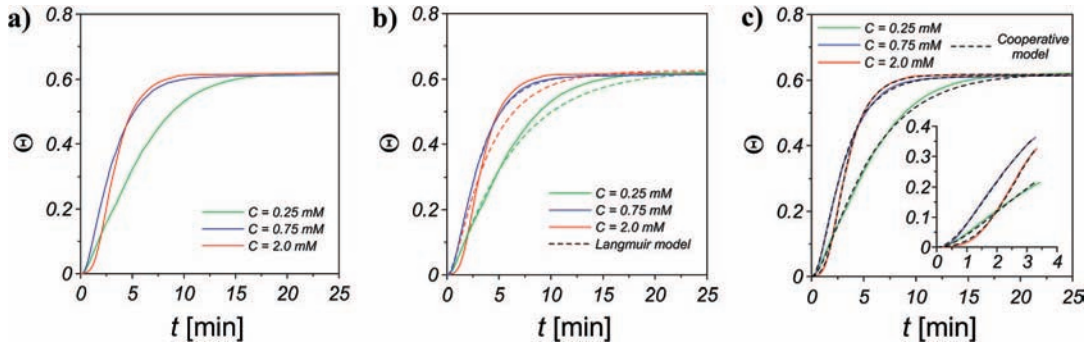

Figure 2. Fractional surface coverage versus time: (a) QCM results, (b) comparison of QCM results (solid lines) and Langmuir model (dashed lines), and (c) comparison of QCM results (solid lines) and cooperative model (dashed lines). The inset zooms in on the early time points. Note that the 2 mM adsorption is initially slower than that from either 0.25 or 0.75 mM solutions.

Experimental Section

Nanoparticles and the Coating Solution. In all experiments, we used gold and silver NPs (6 nm in diameter and dispersity $\sigma = 11\%$), prepared according to the procedure described in refs 14, 15. Positively and negatively charged NPs were prepared by functionalizing AgNPs and/or AuNPs with self-assembled monolayers of, respectively, *N*,*N*,*N*-trimethyl(11-mercaptoundecyl)ammonium chloride (TMA, Figure 1a) and mercaptoundecanoic acid (MUA, Figure 1a). The coating solution of oppositely charged NPs was prepared as descried before.[13] Briefly, MUA NPs were fully deprotonated at pH = 11[14,16,17] and titrated with a solution of TMA NPs (note that titration of TMA NPs with MUA NPs gave identical results) until precipitation at the point when the charges of the nanoparticles were neutralized (i.e., when $\sum Q_{NP+} + \sum Q_{NP-} = 0$). The electroneutral nanoparticle precipitate thus obtained (from 0.5−2 mM solutions in terms of atoms of each metal) was washed several times with water to remove salts, redissolved in deionized water at 60−65 °C, and finally microfiltered to give a stable (for months) 2 mM solution[17] containing oppositely charged NPs in equal proportions. Other NP solutions (0.25 and 0.75 mM) were prepared by direct dilution of the 2 mM solution with deionized water.

QCM-D Experiments. The adsorption studies were performed on a 4-channel QCM-D system (Q-Sense, Glen Burnie, MD), which related the shift from a resonance frequency of the quartz resonator to the mass absorbed onto on the resonator's surface via $\Delta f = -\Delta m/c$ (where $c = 17.7$ ng cm^{-2} Hz^{-1} and Δm is the mass adsorbed per unit area) (Figure 1b). An E4 sample chamber had four removable flow modules, each holding one sensor. The QCM-D instrument measured simultaneously at the fundamental frequency of the sensor crystal (5 MHz) and at the third, fifth, seventh, ninth, 11th, and 13th overtones of this frequency. The multiple measurements gave reliability to the results obtained. In the present study, all flow modules contained 5-MHz quartz sensor crystals coated with silicon dioxide and were used in parallel configuration. Silicon dioxide was cleaned using the following protocol: UV/ozone treatment for 10 min followed by cleaning in a 2% SDS solution for 30 min and rinsing with DI water and, thereafter, UV/ozone treatment for another 10 min.

In the first three modules, solutions of concentrations $C_0 =$ 0.25, 0.75, and 2 mM (in terms of metal atoms) of the chemically modified nanoparticles (1:1 AuNP/AgNP) were pumped over each sensor using a peristaltic pump that gave flow rate $Q = 50$ μL/min. The fourth module was used as a control, where a solution of noncoating nanoparticles (AuMUA) was pumped. Such parallel configuration of flow modules enabled four parallel, real-time, and simultaneous measurements of frequency and dissipation changes for different concentrations of nanoparticles. All measurements were performed at 25 °C.

Fitting. The kinetic models were fitted to the experimental data by minimizing the sum-squared-error between the experimental and calculated surface coverages at all time points. For a given set of rate constants (k_a, k_d for the Lagmuir model; k_1, k_2, k_d for the cooperative model), the kinetic equations were integrated numerically using a fourth-order Runge−Kutta integration scheme with adaptive time-stepping,[18] and the sum-squared-error was computed. This error was then minimized with respect to the unknown rate constants using the simplex search method[19] to give the best-fit values presented here.

Results and Discussion

Figure 2a summarizes the results of the QCM experiments and plots the fractional surface coverage, Θ,[20] of the NP films as a function of time, *t*, for three different concentrations, C_0, of NP solutions. The most notable features of these dependencies are that (i) irrespective of C_0, all curves plateau at the same surface coverage, $\Theta_{max} \approx 62\%$, and (ii) the initial rate of adsorption is not a monotonic function of C_0 and decreases at high NP concentration (compare curves for $C_0 = 0.75$ mM and $C_0 = 2$ mM). In particular, the sigmoidal adsorption curve for $C_0 = 2$ mM suggests that the adsorption process might be cooperative.[21]

To model this process we developed kinetic equations that account for the flow of the NP solution through the sensor and for the adsorption process itself. The flow equation expressing the conservation of NPs in the QCM chamber (see Figure 1b) can be written as

$$\frac{dC(t)}{dt} = \frac{Q}{V}(C_0 - C(t)) - \frac{\Gamma_{max} A}{V}\left(\frac{d\Theta}{dt}\right) \qquad (1)$$

where $C(t)$ is the NP concentration within the chamber at time *t*, C_0 is the concentration of NP solution flowing into the sensing chamber, Q is the volumetric flow rate (50 μL/min), V is the volume of the chamber (40 mm^3), and A is the area of surface onto which particles adsorb (78.5 mm^2), $\Gamma_{max} \approx 1.8 \times 10^{16}$ NPs/m^2 is the maximum surface density of adsorbed NPs, and ($d\Theta/dt$) is the net adsorption rate expressed in terms of the fractional surface coverage, Θ.

The flow equation is coupled to that describing the fractional surface coverage, which evolves due to the adsorption and desorption of NPs onto/from the surface. If this process were not cooperative, one could use the simple Langmuir kinetic model[22] of the form

$$\frac{d\Theta}{dt} = k_a C(t)(1-\Theta) - k_d\Theta \quad (2)$$

where k_a and k_d are the rate constants for NP adsorption and desorption, respectively. The time-dependent surface coverage may then be calculated by solving eqs 1 and 2 simultaneously with initial conditions $\Theta(0) = 0$ and $C(0) = 0$. Figure 2b compares the experimental adsorption curves to those calculated using the best-fit values of the rate constants (k_a, k_d). Not surprisingly, the agreement is generally poor (especially at long times), and the model completely fails to reproduce the kinetics at higher NP concentrations, for which it does not reproduce the characteristic sigmoidal adsorption suggestive of cooperative interactions.

Physically, cooperativity can be attributed to the fact that the already adsorbed particles facilitate adsorption of oppositely charged NPs at neighboring sites (Figure 3a). While, in principle, the degree of such "enhancement" depends on the specific configuration of the NPs on the surface, accounting for all possibilities is prohibitive and unnecessarily complicates the model. Instead, we suggest a simple model that distinguishes only three types of sites: empty and having at least one already adsorbed NP neighbor (site S1), empty and having no neighbors (S2), and occupied (S3). Here, owing to the short-range of the electrostatic interactions,[17,23] a "neighbor" refers to one of the six possible nearest neighbors for hexagonal close packing. Furthermore, we assume that the NPs are randomly distributed on the surface; this simplifying assumption is appropriate when the adsorbed NPs interact only weakly and do not cluster together on the surface. With these assumptions, the probability of finding an occupied site is Θ, an empty site $1 - \Theta$, a site with no occupied neighbors $(1 - \Theta)^6$, and a site with at least one occupied neighbor $[1 - (1 - \Theta)^6]$. Thus, the probabilities, P, of finding the sites of each type for a given surface coverage, Θ, are approximated as $P(S1,\Theta) = [1 - (1 - \Theta)^6](1 - \Theta)$, $P(S2,\Theta) = (1 - \Theta)^6(1 - \Theta)$, and $P(S3,\Theta) = \Theta$. Figure 3b plots these probabilities for different values of surface coverage.

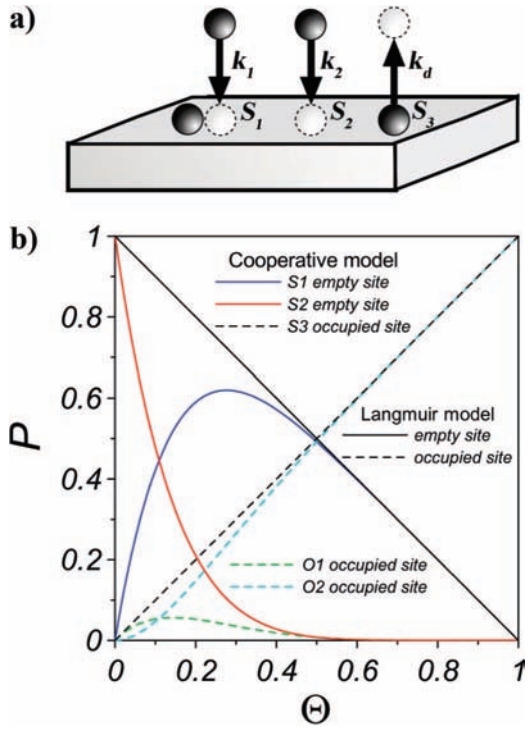

Figure 3. (a) Scheme illustrating different types of sites and adsorption/desorption rates used in the cooperative model. (b) Probabilities of finding different types of sites plotted as a function of the fractional surface coverage. Straight diagonal lines correspond to the simple Langmuir model. Colored lines correspond to the sites used in the cooperative adsorption model. Note that the probability of finding sites O2 (occupied, having no neighbors) is always relatively small, so desorption from such sites can be neglected in the model.

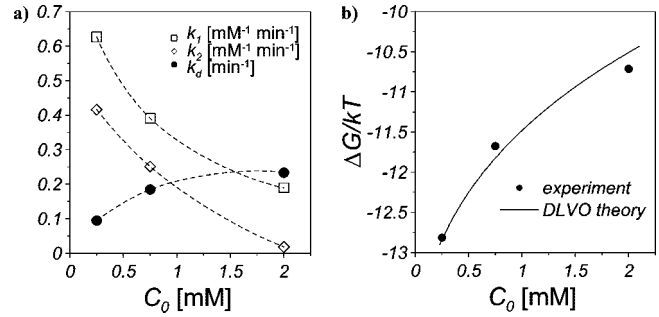

Figure 4. (a) Dependencies of the adsorption (k_1, k_2) and desorption (k_d) rate constants on the concentration of the NP solution, obtained from the cooperative adsorption model. (b) Free energy of NP adsorption as a function of C_0. Markers correspond to values estimated from the experimental rate constants. Assuming $\Delta G \sim U_{surf}$ (see eq 5 in the main text), the line represents the best-fit to data where the net charge, q, was the only fitting parameter (with the fitted value $q = 14.5e$ in very good agreement with experimental estimates, $q = 13-16e$).

With these preliminaries, the adsorption equation may be written as

$$\frac{d\Theta}{dt} = k_1 C(t)[1-(1-\Theta)^6](1-\Theta) + k_2 C(t)(1-\Theta)^6(1-\Theta) - k_d\Theta \quad (3)$$

Note that since the model distinguishes two types of empty sites, S1 and S2, there are now two adsorption rate constants, k_1, k_2, which characterize the degree of cooperativity during adsorption. Specifically, for $k_1 = k_2$, there is no preference between empty sites with and without neighboring NPs (i.e., no cooperativity), and eq 3 reduces to the simple Langmuir adsorption model (eq 2). For $k_1 > k_2$, the adsorption rate is faster onto empty sites with neighbors (positive cooperativity), while for $k_1 < k_2$, the presence of neighboring NPs acts to inhibit adsorption (negative cooperativity). In contrast to the two adsorption processes, eq 3 incorporates only one desorption process (with rate constant, k_d); in other words, there is no distinction between desorption from a site having no neighboring NPs (site O1) and from the site having one or more neighbors (O2). The rationale behind this simplification is that the probability of finding an O1 $[P(O1,\Theta) = \Theta(1 - \Theta)^6]$ site is smaller than that of finding an O2 site $\{P(O2,\Theta) = \Theta[1- (1 - \Theta)^6]\}$ for all but small values of the surface coverage (Figure 3b).

Simultaneous solution of eqs 1 and 3 using the best-fit values of the rate constants (k_1, k_2, k_d) gave adsorption curves that agreed with the experimental ones (Figure 2c). An important result here is that the adsorption rate constants k_1 and k_2 decrease with increasing NP concentrations, whereas the desorption rate, k_d, increases slightly (Figure 4a). Furthermore, the rate constant k_1 is larger than k_2 for all concentrations studied. Thus, the adsorption process is characterized by positive cooperativity, whereby adsorbed particles facilitate the adsorption of more NPs onto the surface.

Furthermore, the relative importance of cooperative versus noncooperative adsorption—as characterized by the ratio k_1/k_2—increases with increasing NP concentration, C_0. For large k_1/k_2 ratios (cf. Figure 4a for $C_0 = 2$ mM), adsorption is

dominated by the cooperative mechanism with the exception of the very initial stages of the process, during which the first particles are "seeded" by the noncooperative mechanism. Following this slow "seeding" process (noncooperative), NPs begin to adsorb increasingly rapidly via the cooperative mechanism. Near the equilibrium coverage, however, the net adsorption rate decelerates due to a decreased availability of open sites and to an increase in the NP desorption rate. Combined, this initial acceleration and ultimate approach to equilibrium create the characteristic sigmoidal curves observed in experiment (cf. Figure 2c).

We observe that the model fits experimental data best for 2 mM AuNPs (as compared to 0.25 and 0.75 mM). This is likely due the strong cooperative effects associated with higher salt concentrations. Specifically, for 2 mM NPs, the ratio k_1/k_2 measuring the relative importance of cooperative adsorption is as large as ~20 (Figure 4a). Thus, the kinetics is dominated by a single adsorption process, i.e., the cooperative one (see the first term of eq 3). The strong agreement with the experimental data in this limit ($k_1/k_2 \gg 1$) suggests that the cooperative mechanism is well-captured by the proposed model. For smaller NP and salt concentrations, however, the k_1/k_2 ratio decreases to less than 2 such that both adsorption processes (i.e., cooperative and noncooperative) are of similar importance. In this more complex case, the model that does not distinguish between specific surface configurations/numbers of neighbors is probably too simplistic and deviates slightly from the experiment.

The k_1 vs C_0 and k_d vs C_0 trends can be rationalized by thermodynamic arguments that apply when the surface coverage approaches its equilibrium value ($\Theta_{max} \approx 62\%$). In this regime, the vast majority of empty sites have NP neighbors and adsorption is dominated by the cooperative term. It follows that the equilibrium constant for NP adsorption may be expressed as $K = [H_2O]k_1/k_d$ ($[H_2O] = 55.5$ M). The observation that k_1 decreases and k_d increases with increasing C_0 is then equivalent to saying that the free energy of adsorption $\Delta G = -k_BT \ln K$ becomes less favorable (i.e., increases) (Figure 4b). Importantly, this conclusion agrees with the predictions of the DLVO theory applied to the NP interactions within the adsorbed monolayer.

NP Interactions in the Adsorbed Layer. As described previously,[13] the free energy of adsorption is due primarily to the difference in the electrostatic energy, U, of NPs in the solution and on the surface $\Delta G \approx U_{surf} - U_{sol}$. In solution, the electrostatic forces between NPs are negligible, since the mean interparticle distance (>100 nm for the unaggregated, dilute solutions used here) is much larger than the screening length ($\kappa^{-1} \sim 10$ nm). Thus, $U_{sol} \sim 0$ and the energy of adsorption is governed only by the electrostatic interactions between NPs and the surface and between NPs on the surface. Importantly, the interactions of positive and negatively charged NPs with the negatively charged subtrate[13] are opposite in sign and roughly equal in magnitude; i.e., they largely cancel one another. Therefore, the main contribution to the energy of adsorption is due to the electrostatic interaction between oppositely charged NPs adsorbed on the substrate.

Specifically, the magnitude of U_{surf} and its dependence on the salt concentration can be approximated by considering the electrostatic energy between two neighboring, oppositely charged NPs. Following the DLVO theory of colloidal interactions, the electrostatic interaction between two oppositely charged particles of net charge q, radius R, and separated by a distance r may be approximated as

$$U_{surf} \approx \frac{-q^2R}{4\pi\varepsilon_0\varepsilon(1+\kappa R)^2}\frac{\exp(-\kappa(r-2R))}{r} \quad (4)$$

where $\kappa^{-1} = (\varepsilon_0\varepsilon k_BT/2C_Se^2)^{1/2}$ is the Debye screening length, C_S is the salt concentration, e is the fundamental charge, ε_0 is the permittivity of a vacuum, ε is the dielectric constant of the solvent, k_B is the Boltzmann constant, T is the temperature. Thus, for two oppositely charged NPs at contact,

$$U_{surf} \approx -q^2/(8\pi)\varepsilon_0\varepsilon R(1+\kappa R)^2 \quad (5)$$

where $q = 14.5e$ was fitted to match the experimental data and agrees well with previous ζ-potential measurements ($\zeta = 40-50$ mV corresponding to $q = 13-16e$).

Importantly, since the solutions were prepared by diluting the same 2 mM NP standard, the salt concentration decreases with the NP concentration as $C_S = N_{ions}/N_{metal}C_0$, where the proportionality factor, N_{ions}/N_{metal}, is the ratio between the number of ions and the number of metal atoms (Au and Ag) in the initial solution; here, $N_{ions}/N_{metal} = 0.079$.[24] Because the screening length scales as $\kappa^{-1} \sim C_S^{-1/2}$, less concentrated NP solutions are characterized by larger screening lengths and by effectively stronger interactions between adsorbed particles (see eq 5) than more concentrated solutions. In other words, U_{surf} and ΔG become less favorable as the concentration of NPs in solution, C_0, increases. Figure 4b shows that this simple DLVO prediction quantified by eq 5 gives a good fit to the values of ΔG estimated from QCM experiments.

Summary

In sum, we used the QCM technique to study the mechanism of surface adsorption from solutions comprising oppositely charged NPs. The model we developed reproduces the experimental data and suggests that the adsorption process is cooperative, in the sense that the particles already present on the surface facilitate the adsorption of NPs from solution. The model also predicts concentration-dependent surface adsorption energies that are consistent with the DLVO theory of colloidal interactions. From a practical point of view, the key finding of this work is that increasing the concentration of the NP solution does not necessarily lead to an increasing rate of adsorption; consequently, less dilute NP solutions might be preferable in real-life coating applications.[13] In the future, it would be interesting to extend the present analysis to mixtures of NPs of different sizes and/or different relative charges.

Acknowledgment. This work was supported by Dow Chemical. B.A.G. gratefully acknowledges financial assistance from the CCNE (Grant No. U54 CA119341). K.J.M.B. was supported by an NSF Graduate Fellowship. The authors thank Dr. Stoyan Smoukov for helpful discussions and for facilitating the collaboration between Northwestern and Q-sense.

References and Notes

(1) Coe-Sullivan, S.; Steckel, J. S.; Woo, W. K.; Bawendi, M. G.; Bulovic, V. *Adv. Funct. Mater.* **2005**, *15*, 1117.
(2) Currie, E. P. K.; Tilley, M. *J. Soc. Inf. Display* **2005**, *13*, 773.
(3) Prevo, B. G.; Hwang, Y.; Velev, O. D. *Chem. Mater.* **2005**, *17*, 3642.
(4) Shen, G. X.; Chen, Y. C.; Lin, C. J. *Thin Solid Films* **2005**, *489*, 130.
(5) Lee, S. W.; Drwiega, J.; Wu, C. Y.; Mazyck, D.; Sigmund, W. M. *Chem. Mater.* **2004**, *16*, 1160.
(6) Chen, S. W. *Langmuir* **2001**, *17*, 2878.
(7) Musick, M. D.; Keating, C. D.; Lyon, L. A.; Botsko, S. L.; Pena, D. J.; Holliway, W. D.; McEvoy, T. M.; Richardson, J. N.; Natan, M. J. *Chem. Mater.* **2000**, *12*, 2869.

(8) Quinn, B. M.; Dekker, C.; Lemay, S. G. *J. Am. Chem. Soc.* **2005**, *127*, 6146.
(9) Zhao, L. Y.; Eldridge, K. R.; Sukhija, K.; Jalili, H.; Heinig, N. F.; Leung, K. T. *Appl. Phys. Lett.* **2006**, 88.
(10) Peng, X. G.; Zhang, Y.; Yang, J.; Zou, B. S.; Xiao, L. Z.; Li, T. J. *J. Phys. Chem.* **1992**, *96*, 3412.
(11) Song, H.; Kim, F.; Connor, S.; Somorjai, G. A.; Yang, P. D. *J. Phys. Chem. B* **2005**, *109*, 188.
(12) Caruso, R. A.; Antonietti, M. *Chem. Mater.* **2001**, *13*, 3272.
(13) Smoukov, S. K.; Bishop, K. J. M.; Kowalczyk, B.; Kalsin, A. M.; Grzybowski, B. A. *J. Am. Chem. Soc.* **2007**, *129*, 15623.
(14) Kalsin, A. M.; Grzybowski, B. A. *Nano Lett.* **2007**, *7*, 1018.
(15) Kalsin, A. M.; Kowalczyk, B.; Wesson, P.; Paszewski, M.; Grzybowski, B. A. *J. Am. Chem. Soc.* **2007**, *129*, 6664.
(16) Leopold, M. C.; Black, J. A.; Bowden, E. F. *Langmuir* **2002**, *18*, 978.
(17) Kalsin, A. M.; Fialkowski, M.; Paszewski, M.; Smoukov, S. K.; Bishop, K. J. M.; Grzybowski, B. A. *Science* **2006**, *312*, 420.
(18) Dormand, J. R.; Prince, P. J. *J. Comput. Appl. Math.* **1980**, *6*, 19.
(19) Lagarias, J. C.; Reeds, J. A.; Wright, M. H.; Wright, P. E. *SIAM J. Optim.* **1998**, *9*, 112.
(20) The surface coverage was calculated as $\Theta = -c\Delta f R^2 (12)^{1/2}/m_{NP}$ where $R = 4.2$ nm is the total NP radius (metal core plus coating SAM) and $m_{NP} = 2.49 \times 10^{-23}$ kg is the mass of one NP.
(21) Evans, J. W. *Rev. Mod. Phys.* **1993**, *65*, 1281.
(22) Fava, A.; Eyring, H. *J. Phys. Chem.* **1956**, *60*, 890.
(23) Bishop, K. J. M.; Grzybowski, B. A. *ChemPhysChem* **2007**, *8*, 2171.
(24) For NPs prepared without any additional salt, the number of ions in solution is directly equal to the number of charged ligands adsorbed on the NPs surface. Here, the ratio between the number of ions and the number of metal atoms is $N_{ions}/N_{metal} = 3\nu/(aR_c)$, where $a = 21.4$ Å^2 is the adsorption area of the ligands,[25] $\nu \approx 17$ Å^3 is the molar volume of bulk Au or Ag, and $R_c = 3$ nm is the radius of the NP's metal core.
(25) Leff, D. V.; Ohara, P. C.; Heath, J. R.; Gelbart, W. M. *J. Phys. Chem.* **1995**, *99*, 7036.

JP809447M